

The Link Between Star Formation and Gas in Nearby Galaxies - Feldmann et al 2020

Justin Bopp

March 2024

Deciphering the process by which galaxies generate their stars stands as a primary objective within the realm of galaxy theory. The identification of a notably strong correlation between the rate of star formation (SFR) and the stellar mass of galaxies shows a tight relationship in the evolution of stars across the majority of star-forming galaxies. Although the exact physical mechanism behind this star-forming sequence (SFS) remains elusive, it is likely that it is associated with the accumulation of gas onto galaxies and the expansion of their parent dark matter halos.

Feldmann et al 2020 used two different samples are used in the present analysis, 1012 galaxies selected from the extended GALEX Arecibo SDSS Survey14 (xGASS) and 54 additional galaxies with molecular gas measurements from the CO Legacy Database for GASS13 (xCOLD GASS) that are not in xGASS. They used a joint distribution of SFRs, neutral gas (NGS), and molecular gas (MGS) masses at fixed M_{star} modeled as a non-Gaussian multivariate distribution with parameters that vary with M_{star} . They employ the Likelihood Estimation for Observational data with Python (LEO-Py) method to compute the likelihood of the various distribution parameters and find the probability distribution of the distribution parameters using the Markov Chain Monte Carlo (MCMC) method. SFRs and gas masses of galaxies in the representative sample are shown in ???. Also shown is the peak position of the SFS (Fig. 1a), the NGS (Fig. 1b), and the MGS (Fig. 1c) as well as their scatter according to their fiducial model. They also plot SFRs, M_{HI} , and M_{H_2} relative to the SFS, NGS, and MGS both for the observational xGASS/xCOLD GASS data and for the intrinsic properties as predicted by their fiducial model. . They find that SFRs, M_{HI} , and M_{H_2} , when measured relative to the peak position of their respective sequences, form an approximately two-dimensional surface, the Star Formation Plane (SFP), that is largely independent of stellar mass suggesting it is an approximately universal characteristic of nearby galaxies.

They show that the slope of the SFR – M_{H_2} relation is directly linked to the (molecular, neutral, total) gas depletion time, t_{dep} , which is defined as the ratio between (molecular, neutral, total) gas mass and SFR. They state that the total gas mass refers to the sum of molecular and neutral gas masses, and t_{dep} corresponds to the time it would take to convert the present gas reservoir

into stars at the current SFR. They show that the gas depletion times are almost constant in normal star-forming galaxies along the SFS. They also show that typical star-forming galaxies suggest that their SFRs are largely driven by their molecular gas masses, rather than stellar masses. They state that while galaxies near the SFS have on average similar molecular gas depletion times, the ratio between M_{H_2} and SFR in any given galaxy can differ significantly from this average value as their model predicts a probability distribution, not a deterministic mapping, between gas mass and SFR. They determine that these considerations suggest an evolutionary model in which the average star formation activity and stellar mass growth of star-forming galaxies is determined by the time evolution of the total gas mass such that:

$$SFR(t) = \frac{M_{gas}(t)}{t_{dep}(M_{star}(t), SFR(t), t)} \quad (1)$$

They suggest $SFR(t)$ links the gas mass of galaxies to their SFR and stellar masses. They state this points to a picture in which physical processes affecting M_{gas} via gas inflows and outflows, such as cosmological gas accretion, hot gas cooling, a galactic fountain, and feedback from stars and black holes regulate the star formation activity and mass growth of typical, nearby galaxies

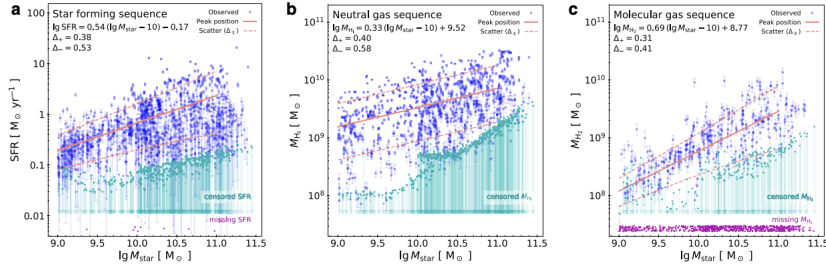


Fig. 1 Scaling relations of nearby galaxies. Slope, normalization, and scatter of the star-forming sequence (a), neutral gas sequence (b), and molecular gas sequence (c). Points show the representative sample based on the xGASS / xCOLD GASS data sets^{13,14}. Specifically, detected SFRs and gas masses are shown as blue circles with error bars indicating measurement uncertainties (one standard deviation). A large fraction of the observational data are either undetected/censored (cyan arrows) or missing (purple dots) necessitating careful modeling to avoid systematic biases. Peak position and scatter of each sequence, as determined by this study, are shown by solid and dashed lines. The peak position is defined as the mode of the conditional probability density of $\lg SFR$, $\lg M_{HI}$, and $\lg M_{H_2}$ given M_{star} . The predicted scaling of the peak position with stellar mass as well as the upward (Δ_+) and downward (Δ_-) scatter of each sequence for $M_{star} = 10^{10} M_{\odot}$ galaxies are listed in the legend of each panel.

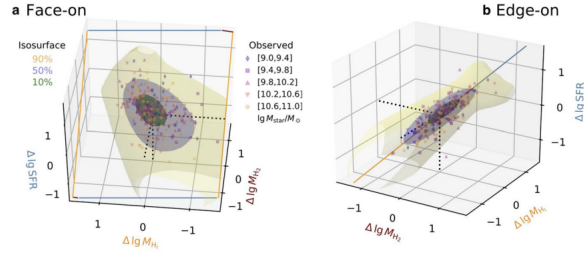


Fig. 2 Star-forming plane. **a** Face-on and **b** edge-on view of the star-forming plane. The star-forming plane refers to the largely two-dimensional distribution of star formation rates (SFRs), neutral and molecular gas masses relative to the peak position of the star-forming, neutral gas, and molecular gas sequence for a given stellar mass. Markers indicate the measured SFRs and gas masses of xGASS/xCOLD GASS observations with marker shapes and colors corresponding to different stellar masses (see legend). Regions bounded by the green, blue, and yellow isosurfaces include 10, 50, and 90% of galaxies (without the zero component) according to the fiducial model. Solid lines mark the intersections of the star-forming plane with the coordinate axes. The orientation of the star-forming plane is calculated via a principal component analysis based on the probability density within the 50% isosurface. The orientation of the star-forming plane is only weakly dependent on stellar mass.

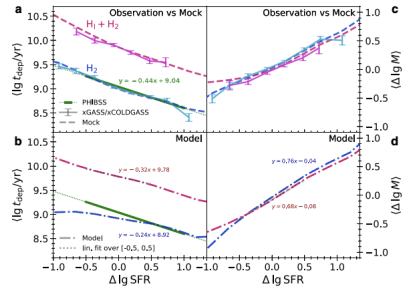


Fig. 4 Scaling of depletion times and gas masses. **a** Average depletion times in the extended xGASS/xCOLD GASS sample of $M_{\text{star}} \sim 10^9\text{--}10^{11}M_{\odot}$ nearby galaxies (solid lines with error bars) and in a mock sample with the same stellar mass distribution (dashed lines) showing good agreement. Blue/cyan lines (red/magenta lines) refer to molecular gas (to the sum of molecular and neutral gas including Helium). Galaxies with undetected or missing star formation rates (SFRs) are excluded from the analysis. Error bars correspond to standard errors of the bin averages. The solid green line shows the fit of the H_2 depletion time from the PHIBSS survey¹⁰ covering $z = 0\text{--}4$ (dotted lines are extrapolations). **b** The scaling of the actual depletion times, i.e., if measured without observational errors and detection limits, for the galaxies in the mock sample. Galaxies with zero SFRs are excluded from the analysis. For typical offsets from the star-forming sequence, the molecular gas depletion time shows only a mild dependence ($\propto \text{SFR}^{-0.24}$) on SFR. **c, d** Same as **a, b** but showing the average change in gas masses relative to the peak position of the corresponding gas sequence with offset from the star-forming sequence. The peak position of the total gas sequence is given by the sum of the peak positions of the molecular and neutral gas sequences including Helium. Changes in star formation activity of typical star-forming galaxies are tightly linked to changes in their molecular and total gas masses.